

## An INDO/S MO Study of Alloxazine and its Monomethyl Derivatives

Henryk Szymusiak,<sup>a,\*</sup> Jerzy Konarski,<sup>b</sup> and Jacek Koziol<sup>a</sup>

<sup>a</sup> Institute of Commodity Science, Academy of Economics in Poznan, Marchlewskiego 146, 60-967 Poznan, Poland

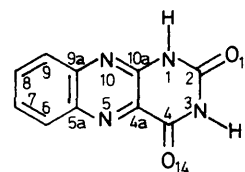
<sup>b</sup> Department of Chemistry, A. Mickiewicz University, Grunwaldzka 6, 60-780 Poznan, Poland

The electronic structure of some monomethyl derivatives of alloxazine has been investigated by the INDO/S-CI-1 method in both the ground and in the two first-excited singlet states. A description of the intrinsic states of molecules by the extensive use of HOMO/LUMO coefficients is suggested. The proposed method both quantitatively and qualitatively characterises satisfactorily various phenomena arising from spectral properties, from reactivity to the interpretation of NMR spectra. The proposed method shows explicitly non-accidental conjunctions, arranging the terms in certain logical sequences between properties of a molecule and of a substituent in its definite site.

The significance of these results is reviewed in relation to the experimentally identified chemical and spectral properties. The influence of substitution by a methyl group on the electronic charge distribution and on the variation of dipole moment, transition moment, orbital energies and electronic transitions are examined. The importance of the frontier parameters of the HOMO/LUMO state in a description of substitution effect is emphasized.

The substitution of a hydrogen atom in the alloxazine molecule causes changes in its physicochemical and spectral properties. The molecule is perturbed in two ways: by resonance (*R*) and by induction (*I*). Both *I* and *R* effects bring about changes in the absorption wavelength and increase the intensity of the absorption bands. Generally, the changes caused by resonance effects are greater than those caused by inductive effects. In the case of the alkyl substituents, an additional effect due to hyperconjugation (Baker–Nathan effect) is observed. As a result of a coupling-type interaction between the binding electrons of the alkyl group and the  $\pi$ -electrons of the molecule this effect relates to positive-resonance interaction (+*R*) of substituents with free electron pairs. In both interactions the direction of electron density flow is the same. This effect has been investigated by Baird.<sup>1</sup> However, practically all these effects are difficult to distinguish quantitatively, thus all considerations should be limited to effects in which the direction of electron density flow is in the opposite sense (–*I*) and (+*R*).

The above-mentioned interactions will serve as key features for the analysis of alloxazine monomethyl derivatives at the semiempirical approach level. Alloxazines are products of the biochemical or photochemical decomposition of biologically active flavins. Many calculations have already been performed on flavins at different levels of approximation. However, alloxazines—because of a lack of crystallographic data—have been considered only marginally. Theoretical investigations on alloxazine have been performed using HMO,<sup>2,3</sup> PPP,<sup>4–6</sup> MINDO/3,<sup>7</sup> CNDO/S,<sup>8</sup> and *ab initio* methods,<sup>9–11</sup> but on account of uncertain geometry the conclusions drawn were rather scant. Our investigation is based on the INDO/S method applied to alloxazine itself and the whole class of its monomethyl derivatives in the hope that the results will offer a better explanation of drastic changes in electronic structure, charge density distribution, and spectral and photochemical properties caused by methyl substitution. Song<sup>3,12</sup> has studied the methyl-substituent effects in isoalloxazines using  $\pi$ -electron semiempirical methods by applying different approaches in the methyl group treatment such as the inductive model, the pseudo-heteroatom approximation and the group-orbital hyperconjugation model. From *ab initio* calculations performed by Clementi *et al.*<sup>13</sup> it is known that for heterocycles the  $\sigma$ - $\pi$



Structure and numbering system of alloxazines.

separability conditions do not hold because of the high polarization of the  $\sigma$ -core. We hope that for a better picture of the changes caused by methyl substitution in the electronic structure of a molecule it will be sufficient to use an INDO/S method involving all valence electrons. The INDO/S method offers a better insight into the structure of electronic transitions which depend partially on the  $\sigma$ -electron framework.

The general aim of the present paper is to show that using frontier parameters taken from HOMO and LUMO states it is possible to explain some of the observed physicochemical properties of the molecules considered.

**Method of Calculation.**—The INDO/S-CI-1 program with original parametrization was applied.<sup>14</sup> The Mataga–Nishimoto parametrization was used for two-electron Coulomb integral calculations. The configuration interaction matrices were constructed of 80 singly excited configurations for alloxazine and its monomethyl derivatives. The extension of the number of singly excited configurations from 60 to 80 did not change the ( $\pi, \pi^*$ ) energy levels and oscillator strengths significantly, but influenced the energy of ( $n, \pi^*$ ) states. Crystal structure geometry is known only for 9-methylalloxazine.<sup>15</sup> For alloxazine itself and its remaining derivatives (6-, 7-, and 8-methylalloxazine), the geometries were obtained by replacing the methyl group by hydrogen for alloxazine, and by replacing the appropriate hydrogen atom in the benzene ring of alloxazine by a methyl group. The bond length  $H_3C-C$  and the orientation of the methyl group with regard to the molecular plane were kept fixed for all the derivatives. The N–H and C–H distances were assumed to be 1.01 and 1.09 Å, respectively.

Application of planar structures obtained by averaging corresponding angles and bond lengths did not give significant

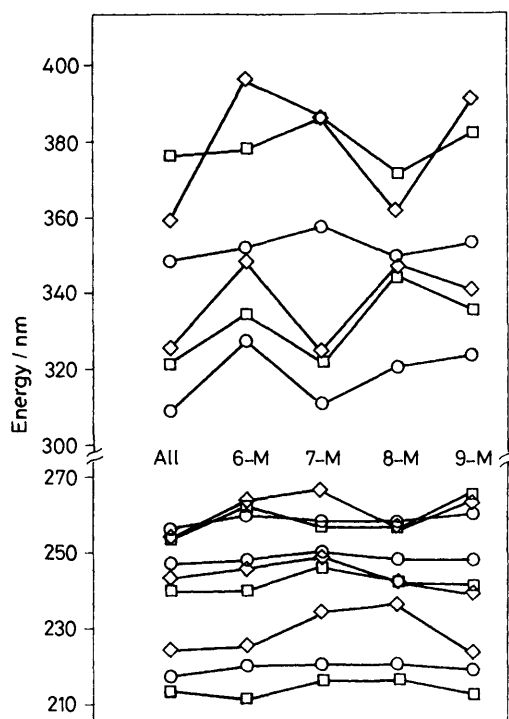


**Figure 1.** The effect of alloxazine methylation on transition energies. Comparison of the results obtained using INDO/S-CI and PPP calculations and experimental measurements.  $\circ$ , INDO/S;  $\square$ , exp;  $\diamond$ , PPP.

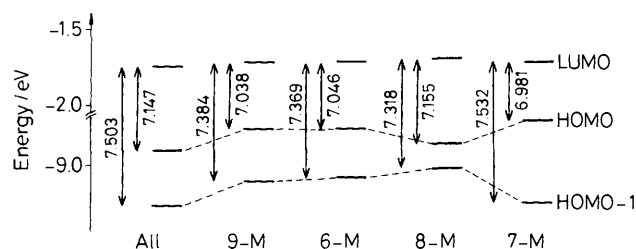


**Figure 2.** The orbital energies of the two highest occupied and the lowest unoccupied MO.

changes in transition energies and other parameters. Computations on the alloxazine framework bent in the N(5)-N(10), C(4a)-C(10a) and C(5a)-C(9a) positions revealed a surprising flexibility in the alloxazine skeleton, although the deviation range from planarity was moderate. Only the two first long-wavelength  $\pi$ - $\pi^*$  transitions ( $S_0$ - $S_1$ , and  $S_0$ - $S_2$ ) are very sensitive to the presence of the methyl group in the benzene ring. With regard to Kasha's rule, these transitions are responsible for the majority of photophysical and photochemical processes. Furthermore, oscillator strengths, dipole moments, electronic dipole transition moments, orbital energies, orbital shapes and charge densities were considered and where possible compared with available experimental data.<sup>4,16,17</sup>

## Results and Discussion

(a) *Electronic Spectra.*—The energies of five  $\pi$ - $\pi^*$  electronic transitions of alloxazine and its monomethyl derivatives, calculated using INDO/S-CI-1 and PPP SCF MO<sup>4,5</sup> and measured experimentally, are compared in Figure 1. Generally, the results obtained by the INDO/S method overestimate the energies for the two first lowest energy  $\pi$ - $\pi^*$  transitions but match the others well. However, qualitative perturbations in the

absorption bands caused by methyl substitution in the benzene ring are reflected pretty well, and the shift directions are correctly reproduced. By comparison with INDO/S, the PPP method reproduces more correctly the experimentally measured transition energies for  $S_0$ - $S_2$  band, but less well for  $S_0$ - $S_1$  and for short-wavelength transitions. The results of the INDO/S calculations are more coherent, thus we have the possibility of a more detailed insight into the electronic structures of the ground state and the two lowest excited states. Distinct vibronic structure is present in the  $S_0$ - $S_1$  band, which means that equilibrium geometries in both states do not differ from each other significantly. In case of the  $S_0$ - $S_2$  band, a lack of well-defined vibronic structure is observed, even in non-polar solvents, which implies greater changes in the molecule's geometry upon excitation to the second singlet-state. It is theoretically possible that the magnitude of the geometry distortions depends on location of the substituent. In spite of this, we may study the relative differences in the electronic structure of particular derivatives in excited states by supposing that these differences result from properties of the ground state and that the interesting pieces of information are concealed in the molecular orbitals. In Figure 2 are shown the orbital energy levels from which originate the two longest wavelength electronic transitions. Both these transitions can be described by single-electron excitations, so the first  $\pi$ - $\pi^*$  transition ( $S_0$ - $S_1$ ) originates from HOMO to LUMO electron promotion whereas the second  $\pi$ - $\pi^*$  transition ( $S_0$ - $S_2$ ) corresponds to electron jump from HOMO-1 to LUMO. By Koopman's theorem<sup>18</sup>  $E(\text{HOMO})$  can be compared with the first ionization potential, and  $E(\text{LUMO})$  with electron affinity. The impact of methylation on  $E(\text{LUMO})$  is relatively small and is in the range 0.01–0.05 eV. In the case of  $E(\text{HOMO})$  and  $E(\text{HOMO}-1)$  the difference is more apparent. Addition of a methyl group tends to increase  $E(\text{HOMO})$  and  $E(\text{HOMO}-1)$ . The energies of the two highest occupied orbitals differ significantly from 0.163 eV in 8-methylalloxazine (almost degenerated) to 0.551 eV in 7-methylalloxazine, resulting in easier oxidation of this compound than of other derivatives (no experimental data for comparison are available). In Figure 2, drastic shifts of the positions of the maxima in absorption spectra of the methyl derivatives, by comparison with unsubstituted alloxazine, are reflected. The largest bathochromic shift of the  $S_0$ - $S_1$  band is observed for 7-methylalloxazine and a small hypsochromic for 8-methylalloxazine; by contrast, a strong bathochromic shift of the  $S_0$ - $S_2$  band takes place in 8-methylalloxazine and no shift in 7-methylalloxazine. Considering the simple orbital excitation model in Figure 3, a linear correlation between orbital energy differences and observed electronic transition energies for all the compounds studied is demonstrated. It appears, however, that a good linear correlation between experimental and theoretical results is obtained only if we assume that the experimental band positions are measured with an error  $< 2$  nm. It is worth noting that measured maxima positions must be treated carefully. It would be better to calculate the gravity-centre of the band (first-order moment). All environmental perturbations influence the oscillation-states distribution of the molecule within a given electronic transition. Mistakes are possible in the case of strongly hidden bands belonging to different transitions which show apparent shifts.

The fairly good correlation between the very complex absorption spectra of alloxazines and the results of semi-empirical calculations confirms the utility of the methods and simple models applied. In addition to these data a more detailed and descriptive analysis of the electronic structure of alloxazine and the changes arising upon its methylation is necessary.

(b) *Ground State Population Analysis.*—In Table 1,  $\sigma$ -electron densities,  $\pi$ -electron densities and net charges for each atom of

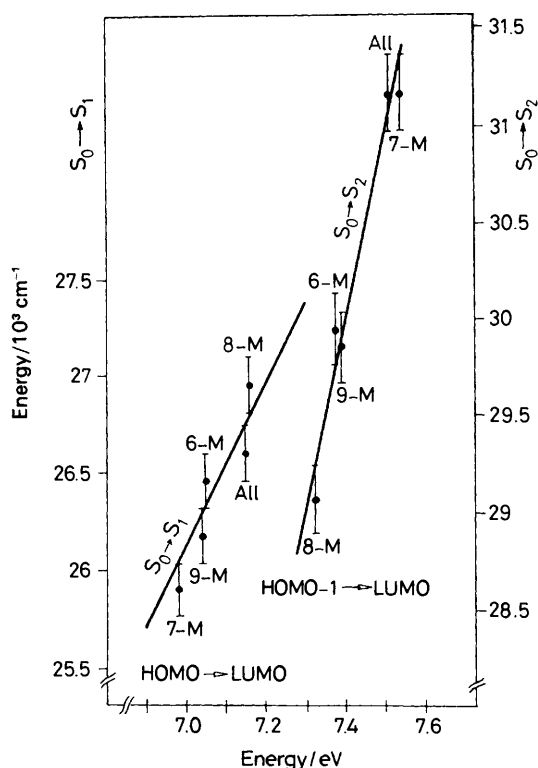


**Figure 3.** Correlation between orbital energy differences (from Figure 2) and observed electronic transition energies. To fit the straight line, each experimental point is expanded up to 4 nm ( $\pm 2$  nm).

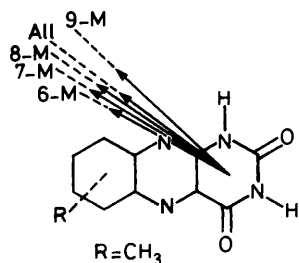


**Figure 4.** Directions of ground state dipole moments (from negative to positive charge centres—from MO calculations). The lengths of arrows are proportional to dipole moment magnitude.

all the compounds studied are summarized. The main changes in electronic structure arising upon methylation, by comparison with unsubstituted alloxazine, will be discussed.

**Alloxazine (All).** The atom the most rich in  $\pi$ -electrons is the C(9) carbon atom which also shows the highest net charge and establishes the most nucleophilic centre in the benzene ring. C(7) seems to be also very reactive. It is interesting to note that C(7) and C(9) have net charges in the ratio  $-0.026 : -0.038$  (2:3) [nitration of alloxazine yields C(7)-NO<sub>2</sub> and C(9)-NO<sub>2</sub> in the ratio 2:3].<sup>2</sup> The most  $\pi$ -electron deficient carbon atoms are C(10a)  $-0.869$  and C(9a)  $-0.918$ ; the net charges are 0.257 and 0.136, respectively. Both atoms constitute the most electrophilic centres in the alloxazine molecule. The  $\pi$ -electron densities of both unsubstituted nitrogen atoms are N(10)  $-1.247$  and N(5)  $-1.127$ ; net charges  $-0.353$  and  $-0.270$ , respectively. It is apparent that N(10) is considerably more reactive towards electrophiles than N(5). The oxygen atom O(12) is relatively richer in electrons than O(14), and their net charges are  $-0.487$  and  $-0.457$ , respectively. The most shielded protons are (in decreasing electron density order) at C(8)  $-0.967$ , C(7)  $-0.963$ , C(9)  $-0.953$ , and C(6)  $-0.951$ : this is

fully consistent with <sup>1</sup>H NMR spectra reported by Grande and Müller.<sup>19</sup> The introduction of a methyl group does not change the electron density on N(3), Me at C(9) does not influence O(14) and Me at C(6) does not influence O(12). The electron densities of all other atoms change upon methylation. The changes in electronic structure caused by methyl group substitution can be described according to the complementarity principle. The chains of atoms connected with C(5a) and C(9a) carbon atoms can be regarded as separate substituents in the benzene ring.

**6-Methylalloxazine (6-MAll).** Substitution at this position enhances the reactivity of C(9) and C(7) [*para* and *ortho* to C(6), respectively] and lowers that of C(8) (*meta*). The methyl group at C(6) is situated *ortho* to C(5a) and *meta* to C(9a). Methyl substitution at C(6) enhances the  $\pi$ -electron density at C(4a), C(5a), and N(10) and lowers it at C(9a), C(10a), N(5), and N(1).

**7-Methylalloxazine (7-MAll).** The methyl group at C(7) enhances the  $\pi$ -electron density and net charge on C(6) and C(8) [both *ortho* to C(7)] and lowers it slightly on C(9). The methyl group at C(7) *para* to C(9a) and *meta* to C(5a) causes a lowering of  $\pi$ -electron density on C(4a), C(5a), N(10), and an increase on C(9a), C(10a), N(5), and N(1).

**8-Methylalloxazine (8-MAll).** The methyl substituent at C(8) increases the  $\pi$ -electron density on C(7) and C(9) [*ortho* positions to C(8)] and lowers it on C(6). The methyl group at C(8) is *para* to C(5a) and *meta* to C(9a). The tendency of the resulting changes are similar but stronger than for 6-MAll, in particular those for nitrogen atoms.

**9-Methylalloxazine (9-MAll).** In this case, enhancement of charge density appears on C(6) [*para* to C(9)] and C(8) (*ortho*) and a lowering on C(7). Other changes are similar to those of 7-MAll, but much weaker because C(7) is *para* to C(9a) and the effect is stronger than in the case of C(9) substitution *ortho* to C(9a). In case of oxygen atoms, apart from the exceptions for 6-MAll and 9-MAll mentioned below, an increase in  $\pi$ -density and net charge is observed at all methyl substitution sites.

The inductive effect causes  $\sigma$ -electron density changes in the opposite direction to that caused by the resonance effect on the  $\pi$ -electron density. The magnitude of the influence of the substituent on  $\sigma$ - and  $\pi$ -electron densities depends on the substitution site. Changes induced in neighbouring substituents, e.g. in the parts attached to C(5a) and C(9a) in the *ortho* position also influence each other. The inductive effect has a rather short-range character, so that  $\pi$ -electron density changes are not fully compensated by changes of  $\sigma$ -density, thus changes in the total electron density occur. It is now obvious why calculations based exclusively on  $\pi$ -electron approximation revealed more dramatic changes in charge density and dipole moments upon methyl substitution.<sup>4,5,17</sup> Our calculations distinctly mark out substitution at the C(7) and C(8) sites. In these alloxazine derivatives the effect of electron density changes are the strongest, but are in opposite directions (see Table 1). From the net charges the overall molecular dipole moments may be computed. The data obtained are given in Table 2 and Figure 4.

The overall molecular dipole moment lies approximately along the N(3)-H bond, which is consistent with the results of *ab initio*<sup>9</sup> and MINDO/3<sup>7</sup> calculations. The value 4.46 D obtained in our calculation for alloxazine is very near to 4.33 D reported by Hall *et al.*<sup>7</sup> For methylated alloxazines only the magnitude of the dipole moments depends significantly upon the methyl group substitution site. It is worth noting that the difference in electronic energy for methylated compounds (Table 2) amounts to *ca.* 140–150 eV (7-MAll or 8-MAll in relation to 6-MAll or 9-MAll). It signifies the energetic importance of the C(7) and C(8) positions. As the substituents with opposite effects mutually strengthen their influence on charge distribution, one can expect a cumulative effect for

**Table 1.** Computed electron densities for selected methyl substituted alloxazines.

Atom	All	6-MAII	7-MAII	8-MAII	9-MAI
N(1)	3.433 <sup>a</sup>	3.434	3.433	3.434	3.433
	-0.203 <sup>b</sup>	-0.202	-0.204	-0.203	-0.204
	1.770 <sup>c</sup>	1.769	1.770	1.769	1.770
C(2)	2.748	2.748	2.748	2.748	2.748
	+0.495	+0.495	+0.495	+0.495	+0.495
	0.757	0.757	0.757	0.757	0.757
O(12)	5.034	5.034	5.034	5.034	5.034
	-0.487	-0.488	-0.488	-0.488	-0.488
	1.454	1.454	1.455	1.454	1.454
N(3)	3.438	3.438	3.438	3.438	3.438
	-0.206	-0.206	-0.206	-0.206	-0.206
	1.768	1.768	1.768	1.768	1.768
C(4)	2.845	2.845	2.845	2.845	2.845
	+0.408	+0.408	+0.408	+0.408	+0.408
	0.747	0.747	0.747	0.747	0.747
O(14)	5.046	5.046	5.047	5.046	5.056
	-0.457	-0.459	-0.458	-0.459	-0.457
	1.411	1.412	1.411	1.412	1.411
C(4a)	2.890	2.889	2.890	2.887	2.890
	+0.139	+0.135	+0.139	+0.134	+0.140
	0.971	0.976	0.970	0.979	0.970
N(5)	4.143	4.143	4.141	4.144	4.143
	-0.270	-0.269	-0.274	-0.269	-0.271
	1.127	1.126	1.133	1.125	1.128
C(5a)	2.926	2.907	2.931	2.922	2.932
	+0.109	+0.105	+0.111	+0.103	+0.110
	0.965	0.988	0.958	0.976	0.959
C(6)	3.035	3.030	3.009	3.042	3.02
	-0.020	+0.030	-0.038	-0.016	-0.031
	0.985	0.941	1.029	0.975	1.004
C(7)	3.032	3.020	3.027	3.016	3.040
	-0.026	-0.049	+0.022	-0.033	-0.025
	0.994	1.029	0.952	1.017	0.984
C(8)	3.040	3.055	3.039	3.040	3.021
	-0.010	-0.011	-0.023	+0.034	-0.029
	0.970	0.957	0.984	0.926	1.008
C(9)	3.022	3.015	3.031	3.005	3.015
	-0.038	-0.052	-0.037	-0.060	+0.012
	1.016	1.037	1.006	1.054	0.973
C(9a)	2.947	2.946	2.938	2.953	2.936
	+0.136	+0.140	+0.139	+0.137	+0.127
	0.918	0.914	0.929	0.910	0.937
N(10)	4.107	4.106	4.108	4.106	4.108
	-0.353	-0.354	-0.352	-0.357	-0.353
	1.246	1.248	1.244	1.251	1.246
C(10a)	2.874	2.875	2.872	2.875	2.873
	+0.257	+0.258	+0.253	+0.258	+0.254
	0.869	0.867	0.876	0.867	0.872
H-C(6)	0.951	—	0.953	0.951	0.953
H-C(7)	0.963	0.966	—	0.964	0.964
H-C(8)	0.967	0.968	0.968	—	0.969
H-C(9)	0.953	0.954	0.953	0.955	—
C-H(3)	—	3.041	3.043	3.042	3.033
—	—	-0.043	-0.045	-0.046	-0.038
—	—	1.002	1.002	1.004	1.005
H(1)	—	0.971	0.982	0.985	0.983
H(2)	—	0.972	0.972	0.970	0.969
H(3)	—	0.967	0.968	0.967	0.966

<sup>a</sup>  $\sigma$ -Electron density. <sup>b</sup> Net charge. <sup>c</sup>  $\pi$ -Electron density. (Net charges are given in units of electrons; '+' means a deficiency of electrons and '-' means an excess of electrons as compared with the isolated atomic state.)

complementary substitutions. Substitution at C(7) and C(8) should therefore give the largest enhancement of electronic density on N(5), N(10), and N(1) and an enhancement of the reactivities of the C(6) and C(9) positions. It is well known that the hydrogen peroxide oxidation of substituted alloxazines yields N(10)-O oxides preferentially over N(5)-O oxides (which

in fact are not formed).<sup>2</sup> It is apparent that N(10) is considerably more reactive towards electrophiles than is N(5), and in particular, substitution at C(8) is preferable. Indeed, 7,8-dimethylalloxazine (so-called lumichrome) is a well known photoproduct of flavins.<sup>17</sup> Similarly strong effects are expected for 8,9- and 6,7-dimethylalloxazines (isolumichromes).

**Table 2.** Electronic energies/eV and dipole moments/D for ground and excited states.

	All	6-MAll	7-MAll	8-MAll	9-MAll
Electronic energy	-13 657.4	-15 279.3	-15 127.6	-15 131.7	-15 268.9
Dipole moments in S <sub>0</sub> state	4.46	4.26	5.08	5.11	4.74
Dipole moments in S <sub>1</sub> state	6.39	8.47	8.00	6.85	7.78
Dipole moments in S <sub>2</sub> state	12.86	10.96	12.52	14.22	12.57

**Table 3.** Correlation between the INDO/S eigenvectors of some substituted alloxazines with those of the unsubstituted alloxazine nucleus

	6-MAll	7-MAll	8-MAll	9-MAll
HOMO	-0.9013	-0.9968	-0.9454	-0.9335
HOMO-1	-0.8922	0.9997	-0.9368	-0.9257

### Magnetic Resonances

It is interesting to compare our results with <sup>1</sup>H and <sup>13</sup>C NMR spectra. The <sup>1</sup>H NMR resonances of alloxazines have not been studied in detail.<sup>19</sup> We can only compare data for All, 7-MAll, 8-MAll, and 7,8-dimethylalloxazine in order to check the cumulative effect. In the case of alloxazine itself a relatively good correlation was found between the electron densities at the aromatic protons and carbon atoms under consideration and the proton chemical shifts. It seems that in order to obtain a better correlation one would require H-C bond length optimization. The shifts induced on the neighbouring aromatic proton resonances by methyl substitution in the benzene ring are proportional to the calculated electron densities in relation to the neighbouring carbon atoms. The introduction of a methyl group at C(7) produces about the same shift for H-C(6) and H-C(8) as the introduction of Me at C(8) for H-C(9) and H-C(7)—*ca.* 20 and 10 ppm, respectively. The chemical shifts of protons in the *meta* position to a substituted carbon atom are smaller, but are in contrast with the calculated electron density decrease at the carbon atoms to which the protons are attached. Complementary substitution at C(7) and C(8) gives the strongest effect on both C(6) and C(9) atoms. The NMR resonances of Me-C(7) and Me-C(8) do not differ significantly, and the <sup>13</sup>C NMR chemical shifts of both methyl carbon atoms are very close, with the C(8) resonance *ca.* 3 ppm more downfield shifted than C(7). Unfortunately, not all assignments are unequivocal in the <sup>13</sup>C NMR spectra,<sup>20</sup> in particular those for C(5a) and C(9a) of alloxazines. The data available for alloxazines singly substituted at C(7), C(8), and 7,8-dimethylalloxazine show rather poor correlation with calculated electron densities. Grande and Müller<sup>20</sup> noticed that the *para* shift on C(9a) when going from All to 7-MAll is only -0.6 ppm, while the *meta* shift on C(9a) (from All to 8-MAll) is larger. We have found a relatively good correlation of C(6), C(7), C(8), and C(9) resonances with calculated  $\pi$ -electron densities for alloxazine. The resonances of the C(8) carbon of alloxazine appears at significantly lower field than others, and that of C(9) is *ca.* 6.5 ppm upfield shifted, which agrees well with  $\pi$ -electron densities (Table 1). Furthermore, in 7-MAll the C(6) carbon atom (*ortho*) is shifted upfield, C(8) (also *ortho*) downfield, and C(9) (*meta* position) upfield. No consistency exists between the observed chemical shifts in this region. The difference between C(2) and C(4) of *ca.* 9 ppm is in agreement with the calculated net charge densities giving values lower by 0.1 e for the C(2) atom. At quaternary carbon atoms C(4a), C(5a), C(9a), and C(10a) no correlation exists. The published electron densities calculated by MINDO/3<sup>7</sup> and *ab initio*<sup>9</sup> methods do not correlate as well. The difference between the resonances of

C(5a) and C(9a) and the resemblance of C(4a) and C(10a) is not reflected by any of the methods used, if we take into account partial charges or  $\pi$ -electron densities. Perhaps the methods applied do not recognize the suggested polarization of the alloxazine by both carbonyl groups exerting their influence *via* the  $\pi$ -electronic system.<sup>20</sup> Unfortunately we do not have precise <sup>13</sup>C NMR data for 6-MAll and 9-MAll. The results of CNDO/S calculations performed by Tokuhiko and Fraenkel<sup>21</sup> for azines using excitation energies of the lower excited states to estimate the local dia- and para-magnetic contributions of the screening constant in <sup>13</sup>C and <sup>14</sup>N NMR spectroscopy showed the very important role played by the actual electronic structure of the excited states of the molecule. The components of the tensor of the local paramagnetic part involve direct information about the excited states of the system through orbital energies.<sup>22</sup> The discrepancies in <sup>13</sup>C chemical shifts due to the substitution site for 7- and 8-MAll can probably be explained by the differences in *E*(HOMO) and *E*(HOMO-1) orbital energies, as shown in Figure 2. It seems that this effect can sometimes dominate the complementarity principle. Such discrepancies in <sup>13</sup>C NMR chemical shifts were not observed in isoalloxazines,<sup>20</sup> where orbital energies are closer together for all methylated derivatives.<sup>7</sup> Hitherto both the dia- and para-magnetic parts have been dependent on orbital shapes, and such differences will be discussed below. As regards electronic density distribution, <sup>13</sup>C NMR resonances are more sensitive to small geometrical parameter changes and to anisotropy of charge distribution in the region of the atom under consideration than to the statistical electron density of the given atoms. It is necessary to look for another simple index involving the anisotropy of charge distribution, particularly in heterocycles because of the high polarization of their  $\sigma$ -core.

(c) *Excited States.*—The resonance effect of the methyl group at particular positions has a distinct influence on the shapes of the two highest occupied molecular orbitals HOMO and HOMO-1, which are  $\pi$  orbitals. The first unoccupied molecular orbital LUMO is relatively less sensitive to substitution in all derivatives; the corresponding atomic orbital coefficients are very similar. The highest coefficients in the HOMO for alloxazine are located primarily at N(1) and then in the quinoxaline moiety. The coefficient for C(7) is the highest and for C(8) the lowest in the benzenoid part of the molecule. The second highest  $\pi$  orbital, HOMO-1, involves mainly O(14), N(10)-N(5)-C(4a) and C(5a)-C(6)-C(7)-C(8)-C(9); here the coefficient for C(7) is much smaller than for other carbon atoms in the benzoic part. In the LUMO orbital the highest probability concentration is on the N(5)-N(10) nitrogen atoms [for N(5) it is much higher], but C(4a), C(9a), C(6), and C(8) and the C=O(14) carbonyl group also have significant shares. To give a mathematical measure of molecular orbital shape changes, the scalar products of proper eigenvectors of unsubstituted and substituted alloxazine were calculated. For the scalar products only 64 functions, 2s and 2p of the atoms of the alloxazine skeleton, were taken into consideration. Atomic orbital coefficients of the methyl groups and the remaining hydrogen atoms were neglected so as to obtain eigenvectors of the same atomic orbital basis (Table 3).

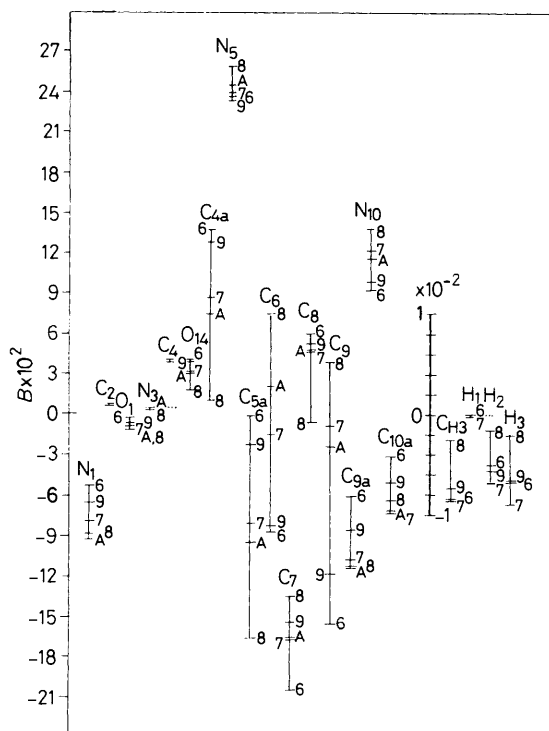


**Figure 5.** Differences between frontier orbital densities ( $C_r^{LUMO})^2$  and frontier electron densities ( $C_r^{HOMO})^2$ , where  $C_r^{LUMO}$  is the LCAO expansion coefficient of the lowest empty MO at atom  $r$  and  $C_r^{HOMO}$  corresponds to the highest occupied MO. Values for methyl substituents are shown in the right-hand section using an expanded scale.  $\beta = (C_r^{LUMO})^2 - (C_r^{HOMO})^2$ .

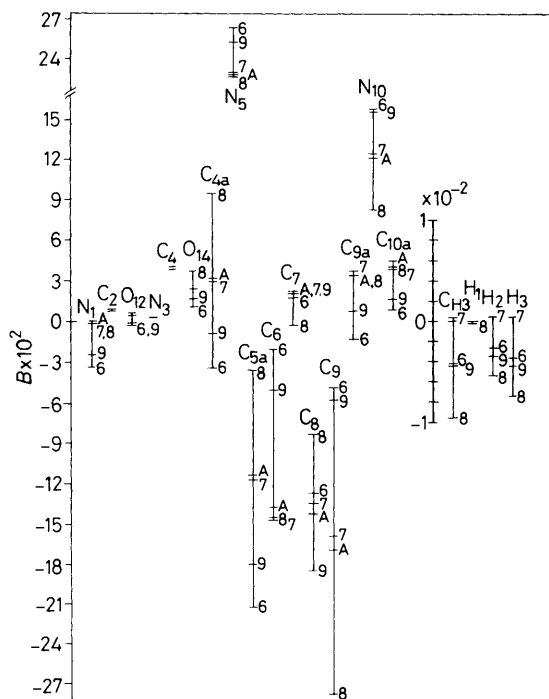


**Figure 6.** As in Figure 5 but for  $C_r^{HOMO-1}$ .

From the data presented in Table 3 it can be seen that methyl groups hardly affect  $\pi$  orbital shapes. A correlation near one-to-one appears only for 7-MAll, and most perturbed orbitals are those of 6-MAll. Scalar products of eigenvectors, *e.g.*

the HOMO of alloxazine and HOMO-1 of its methylated derivatives have also non-zero values, so the mixture of other orbitals in the two highest occupied orbitals upon substitution is not negligible. It proves the higher aromaticity of the alloxazine molecule by comparison with 'parent' isoalloxazines, which was confirmed by Ewig's CNDO/S calculations<sup>8</sup> and investigations of the <sup>1</sup>H NMR spectra.<sup>19</sup> The resonance effect also introduces  $\pi$ - $\sigma$  mixing caused by the presence of methyl groups. Figures 5 and 6 show the detailed dynamics of the calculated first two electronic transitions of alloxazines. The differences between the squares of the LCAO expansion coefficients for particular alloxazine skeleton atoms and of individual methyl groups have been used, considering the dominating molecular orbitals in a given electronic transition. The squares of the coefficients of the HOMO and LUMO are known as Fukui indexes for an incoming electrophile or nucleophile.<sup>23,24</sup> The upper parts of Figures 5 and 6 represent the increment of  $\pi$ -electron density on excitation, and the lower parts adequately correspond to its decrease. In the case of carbon atoms of methyl groups the decrease in electronic density relates to  $2p_z$  or pseudo- $\pi$  of hydrogen atoms (if we assume that a lack of hyperconjugative effect is responsible for this).

**$S_0$ - $S_1$  Transition.** In Figure 5 the differences between the squares of the LUMO and HOMO coefficients (differences between the Fukui indexes) are presented. They express the change in  $\pi$ -electron density on the atoms during excitation. For all the derivatives the changes of  $\pi$ -electron density at N(3), C(2), and C(4) are the same. The characteristic feature is the change of  $\pi$ -electron density which appears in the following order: 8-MAll > All > 7-MAll > 9-MAll > 6-MAll with reference to O(12), O(14), N(1), N(5), N(10), and quaternary carbon atoms C(4a), C(5a), and C(9a). For alloxazine, the  $\pi$ -electron density decreases on C(7) and C(9), increases on C(6) and C(8), and for 8-MAll it decreases on C(7), C(8) and increases on C(6) and C(9). In 6-, 7-, and 9-MAll a decrease in electron density on C(6), C(7), C(9), and an increase on C(8) is observed. The results obtained provide an explanation of the greater reactivity of 8-MAll than of All and 7-MAll.<sup>17</sup> The experimental efficiency of alloxazine-isoalloxazine phototautomerism shows the same tendency. The driving force of the phototautomerism is the charge redistribution between N(10) and N(1) upon excitation.<sup>5,17,25</sup> The phototautomeric effect also depends on the  $pK_a^*$  values for N(1) deprotonation. Quite a good correlation is found between the succession of charge decrease on N(1) with given  $pK_a^*$  values (see Table 3, ref. 17). The  $pK_a^*$  values increase in the order: All -2.3, 8-MAll -2.7, 7-MAll -3.7, 9-MAll -4.0, and 6-MAll -4.7. This order is well predicted by the calculated changes in charge density (see Figure 5). The  $pK_a^*$  values for N(3) deprotonation are very close to the ground state values, in agreement with our results. We have previously concluded that lumichrome (7,8-dimethylalloxazine) should have the greatest change in  $\pi$ -electron density at the nitrogen atoms, therefore we can deduce that lumichrome should have the lowest  $pK_a^*$  value and the highest phototautomeric efficiency of all dimethylated derivatives. It does, in fact, fit the experimental data and the  $pK_a^*$  value is near to that of 7-MAll.

The methyl group at C(7) has the greatest contribution of  $\sigma$ -density to the highest  $\pi$  orbital and at C(8) the lowest. The magnitudes of these contributions correspond to proper absorption band shifts, *e.g.* the lowest energy band in the 7-MAll spectrum is the most bathochromically shifted.<sup>4,16</sup> This can serve as an illustration of the influence of a methyl group hyperconjugative effect on the absorption spectra. The above remarks are reflected in Figure 7, in which the calculated electric dipole transition moments are shown. The magnitudes and directions are arranged in the order 8-MAll, All, 7-MAll, 9-MAll, 6-MAll. In contrast with the results of PPP calcu-

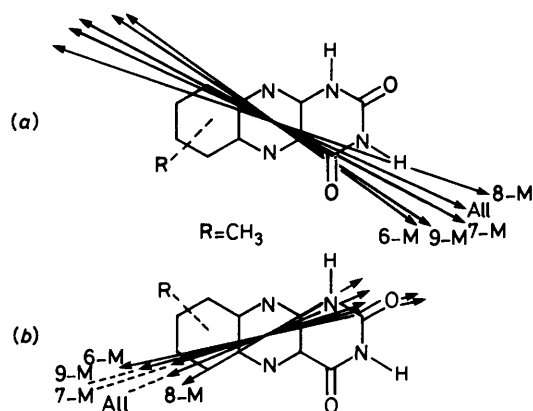


**Figure 7.** Calculated transition moments and directions to the first-excited singlet state (a) and to the second-excited singlet state (b). The arrow lengths are proportional to the magnitude of transition moments.

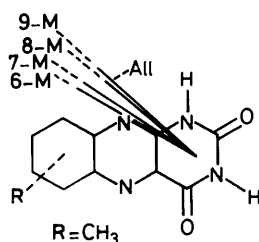


**Figure 8.** Calculated dipole moment vectors of alloxazines in the first-excited state S<sub>1</sub>( $\pi$ ,  $\pi^*$ ) in the CI scheme.

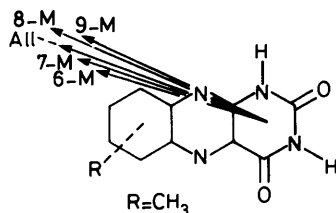


**Figure 9.** Calculated dipole moment vectors of alloxazines in the second-excited state S<sub>2</sub>( $\pi$ ,  $\pi^*$ ).

lations,<sup>4</sup> the directions of the transition moments obtained do not show dramatic changes, all transitions being rather long-axis polarized. The transition moment for 8-MAll forms the smallest angle in relation to the molecule's long axis, but the vector is the largest, and again the transition moment of 6-MAll is the smallest, forming the largest angle with the long axis but remaining still rather long-axis polarized. In addition the directions of the dipole moments (see Figure 8), do not differ much in the first-excited state. In relation to the ground state the magnitudes of the dipole moments are the highest for 6-MAll and 9-MAll which is in agreement with the observation that for these compounds the first absorption band is the most solvent-polarity sensitive.<sup>17</sup>

**S<sub>0</sub>-S<sub>2</sub> Transition.** This transition is promoted from the HOMO-1 orbital to LUMO as the dominating configuration (CI coefficient *ca.* 0.9). From Figure 6 it can be seen that the structure of this transition is very different from S<sub>0</sub>-S<sub>1</sub>. It may arise from the orthogonality of  $\pi$  orbitals which promotes the electron jumping to the same LUMO orbital. In this transition the greatest changes in  $\pi$ -electron density on the N(1), N(5), and N(10) nitrogen atoms are observed for 6-MAll and 9-MAll. All compounds do not differ in  $\pi$ -electron density changes on atoms N(3), C(2), and C(4). On N(5) and N(10) the strongest increment of  $\pi$ -electron density appears for 6-MAll, 9-MAll, 7-MAll, All and the weakest for 8-MAll; the  $\pi$ -electron density on N(1) also

decreases in the same order but is *ca.* 2.5 times less than for the S<sub>0</sub>-S<sub>1</sub> transition. On oxygen and quaternary carbon atoms the succession of  $\pi$ -density changes is the opposite of that observed for the S<sub>0</sub>-S<sub>1</sub> transition. In all derivatives a decrease in electronic density on C(6), C(7), C(9), and an increase on C(7) is observed. The hyperconjugative effect also appears here but in the opposite order as compared with the first transition. The methyl group in 8-MAll now has the largest share in the HOMO-1 orbital (strongest bathochromic effect) and in 7-MAll the smallest (no apparent shift).<sup>4,16,17</sup> The magnitudes of these transition moments (Figure 7) agree well with all conclusions related to charge redistribution during the transition. The directions of these transition moments and those of S<sub>0</sub>-S<sub>1</sub> reveal approximately mirror symmetry with regard to the long axis of the molecule. The lengths of vectors are proportional to the magnitude of changes in  $\pi$ -electron density, *e.g.* on N(5) (similar to the S<sub>0</sub>-S<sub>1</sub> transition). In addition, the directions of dipole moments in the S<sub>2</sub>( $\pi$ ,  $\pi^*$ ) state are very close (Figure 9). In the second-excited state the highest change of dipole moment in relation to the ground state value is observed for 8-MAll (see Table 2). It is known from the experiments that the second band in the 8-MAll spectra is the most sensitive to solvent polarity.<sup>17</sup> It seems that the solvent effects are controlled more by dipole-dipole interactions of the dissolved compound and solvent molecules than by quasi-chemical bonds with the reactive centres of the molecule. Similar remarks based on INDO/S studies on isoalloxazines were formulated by Zuccarello *et al.*<sup>26</sup> The calculated values of dipole moments are very close to each other and are second-order with respect to the solvent effects observed for differently methylated alloxazines.

***n*- $\pi^*$  Transitions.** The calculated energies of *n*- $\pi^*$  transitions are the lowest. For alloxazine the first *n*- $\pi^*$  transition appears at 375 nm, for 6-MAll and 9-MAll at 370 nm and for 7- and 8-MAll at 365 nm. We expected here to observe a hypsochromic effect on methyl substitution; in fact the magnitude of the shifts agrees with the complementarity principle discussed earlier. Lack of experimental confirmation of the presence and localization of *n*- $\pi^*$  transitions (very small oscillator strengths) in this spectral region makes further discussion fruitless.

The attempts to correlate *n*- $\pi^*$  transition energies calculated by INDO/S with observed quantum yields of fluorescence in the presence of other possible channels of deactivation from excited states seem to be difficult and remain unsuccessful.

## Conclusions

MO calculations (INDO/S) using the crystal-structure geometry of 9-methylalloxazine were performed on oxidized alloxazine and related monomethylated alloxazines. Molecular properties resulting from substituent effects have been computed and interpreted in terms of a set of frontier parameters taken from HOMO/LUMO states. The nature of the substituent effect is discussed in terms of its influence on  $\sigma$ - and  $\pi$ -electron density distribution (inductive and resonance effects, respectively) in the ground state as well as on the orbital energies and MO coefficients. It is emphasized, where possible throughout the paper, that *I* and *R* effects appear in different proportions depending on the location of the substituent on neighbouring atoms (*ortho*, *meta*, or *para* in relation to the substitution site) and how these effects are revealed in the properties of ground and excited states. Close agreement with UV spectra, NMR spectroscopy, alloxazine-isoalloxazine phototautomerism efficiency and  $pK_a^*$  for N(1)-H and N(3)-H deprotonation is obtained. A fair correlation was achieved between orbital energies and experimental electron  $\pi$ - $\pi^*$  transitions by omitting the accompanying solvent effects and the intrinsic error of the semiempirical method [Part (a)].

Electron distributions are considered in terms of complementary substitutions and are then compared with available NMR data. It is supposed that discrepancies in  $^{13}\text{C}$  spectral behaviour can be explained by orbital energy and orbital coefficient differences demonstrated here [Part (b)]. The structures of the first two  $\pi-\pi^*$  transitions are described as differences of the Fukui indexes, which are able to show a full picture of electron density redistribution in both excited singlet states. The charge density redistribution between N(1) and N(10) in the first-excited state is important as a driving force for the phototautomerism of alloxazines, showing the highest values in the order: 8-MA11 > All > 7-MA11. Also, the tendency of  $\text{p}K_{\text{a}}^*$  values for the N(1)-H deprotonation is correctly reproduced. The calculated transition moments to both excited states show relatively large specificity of particular derivatives corresponding to different charge changes on the nitrogen atoms. The different sensitivities observed to environmental influences for each methylated alloxazine are reflected by significant differences in dipole moments [Part (c)]. A lot of calculated molecular parameters are still waiting for experimental examination. The results obtained allow us to conclude that extended use of INDO/S MO parameters may serve as good guidance in further investigations of many current problems in the photochemistry of alloxazines.

#### Acknowledgements

The authors thank Professor Dr. J. S. Kwiatkowski of the N. Kopernicus University in Torun, Poland, for stimulating discussions; Dr. A. J. Wisor of the Silesian University in Katowice, Poland; and Dr. J. Waluk of the Institute of Physical Chemistry of the Polish Academy of Sciences in Warsaw for modified computer programs of flexible semiempirical calculations. This work was supported in part by Project CPBP.01.12. PAN.

#### References

- 1 N. C. Baird, *Theor. Chim. Acta*, 1979, **16**, 239.
- 2 P. S. Song and M. Sun, *Chem. Biochem. React., Jerusalem Symp. Quantum. Chem. Biochem.*, 1974, **7**, 407.
- 3 P. S. Song, *Int. J. Quantum Chem.*, 1969, **3**, 303.
- 4 J. Koziol and A. Koziolowa, in 'Flavin and Flavoproteins;

- Physicochemical Properties and Function,' ed. W. Ostrowski, Polish Scientific Publ., Warsaw-Cracow, 1977, p. 81.
- 5 J. Koziol and P. S. Song, unpublished data.
  - 6 K. Nishimoto, *Bull. Chem. Soc. Jpn.*, 1967, **40**, 2493.
  - 7 L. H. Hall, B. J. Orchard, and S. K. Tripathy, *Int. J. Quantum Chem.*, 1987, **31**, 195; 1987, **31**, 217.
  - 8 J. K. Eweg, 'On the Electronic Structures of Free and Protein-Bound Isoalloxazines.' Thesis, Agricultural University of Wageningen, 1982.
  - 9 R. J. Platenkamp, M. H. Palmer, and A. J. G. Visser, *Eur. Biophys. J.*, 1987, **14**, 393.
  - 10 M. H. Palmer and R. J. Platenkamp, in 'Catalysis in Chemistry and Biochemistry. Theory and Experiment,' ed. B. Pullman, D. Reiolel, Dordrecht, The Netherlands, 1979, 147.
  - 11 M. H. Palmer, J. Simpson, and R. J. Platenkamp, *J. Mol. Struct.*, 1980, **66**, 243.
  - 12 P. S. Song, *J. Korean Chem. Soc.*, 1972, **16**, No. 3, 119.
  - 13 E. Clementi, H. Clementi, and R. Davis, *J. Chem. Phys.*, 1967, **46**, 4725.
  - 14 J. E. Ridley and M. C. Zerner, *Theor. Chim. Acta*, 1973, **32**, 111; 1976, **42**, 223.
  - 15 J. Csoeregh, P. Kierkegaard, J. Koziol, and F. Müller, *Acta Chem. Scand., Ser. B*, 1987, **41**, 383.
  - 16 J. Koziol, A. Koziolowa, J. Kociarski, D. Panek-Janc, and J. Dawidowski, *Flavins and Flavoproteins—Proceedings of the 6th International Symposium on Flavins and Flavoproteins*, eds. Kunio Yagi and Toshio Yamano, University Park Press, Baltimore, 1979, p. 475.
  - 17 A. Koziolowa, *Photochem. Photobiol.*, 1979, **29**, 459.
  - 18 T. Koopmans, *Physica (Utrecht)*, 1934, **1**, 104.
  - 19 H. J. Grande, C. G. van Schagen, T. Jarbandhan, and F. Müller, *Helv. Chim. Acta*, 1977, **60**, 348.
  - 20 H. J. Grande, R. Gast, C. G. van Schagen, W. J. H. van Berkel, and F. Müller, *Helv. Chim. Acta*, 1977, **60**, 367.
  - 21 T. Tokuhira and G. Fraenkel, *J. Am. Chem. Soc.*, 1969, **91**, 5005.
  - 22 J. A. Pople, *J. Chem. Phys.*, 1962, **37**, 53.
  - 23 K. Fukui, T. Yonezawa, C. Nagata, and H. Shinga, *J. Chem. Phys.*, 1954, **22**, 1433.
  - 24 K. Fukui, T. Yonezawa, and H. Shinga, *J. Chem. Phys.*, 1952, **20**, 722.
  - 25 J. Komasa, J. Rychlewski, and J. Koziol, *J. Mol. Struct.*, 1988, **170**, 205.
  - 26 F. Zuccarello, G. Buemi, and A. Raudino, *J. Chem. Soc., Faraday Trans. 2*, 1986, **82**, 679.

Paper 8/04666B

Received 25th November 1988

Accepted 14th July 1989